Research Article

Supporting Information

üstalnable

Chemistry & Engineering

Semicontinuous Aqueous Acetone Organosolv Fractionation of Lignocellulosic Biomass: Improved Biorefinery Processing and **Output**

Arjan T. Smit,* Michiel Hoek, Petra A. Bonouvrie, André van Zomeren, Luke A. Riddell, and Pieter C. A. Bruijnincx



ACCESS I

Cite This: ACS Sustainable Chem. Eng. 2024, 12, 4731–4742

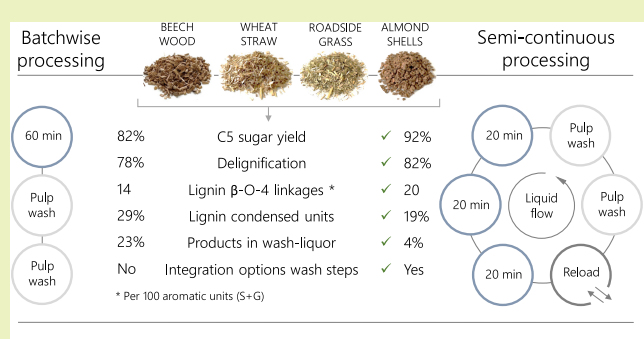
III Metrics & More



Article Recommendations

ABSTRACT: Aqueous acetone organosoly fractionation of the lignocellulosic biomass using a batchwise operation is a robust technology option to produce cellulose, sugars, and lignin. Such fractionation is typically characterized by fast solubilization of most of the lignin and hemicellulose sugars in the early stages of the process, gradually followed by slower removal of the remaining, more recalcitrant part at later stages. As a result, most of the solubilized sugars and lignin experience a relatively long residence time in the hot liquor, leading to undesired sugar degradation and lignin depolymerization-condensation reactions. A lab-scale, semicontinuous countercurrent flow fractionation design is presented

here as a solution to this issue and studied as an intermediate step toward an envisioned scaled-up design involving a series of



Semi-continuous processing improves overall process efficiency and product quality

percolation reactors coupled for liquid exchange. Counter-current semicontinuous processing (SCP) reduces the overall residence time of the solubilized sugars and lignin. While even slightly improving on fractionation performance, i.e., sugar and lignin solubilization, most importantly, SCP resulted in less sugar degradation and more hemicellulose oligomers compared to the simple batch process. SCP lignin proved to be of higher quality with increased β -O-4 content and, consequently, a higher abundance of lignin aliphatic hydroxyl groups, less formation of Hibbert ketones, and reduced condensation. The more native nature of the lignin is reflected in its improved reactivity in reductive partial depolymerization to lower molar mass and dispersity lignin building blocks. Overall, SCP thus provides a powerful and scalable strategy for improving the efficiency and effectiveness of aqueous acetone organosolv fractionation.

KEYWORDS: biomass organosolv pretreatment, semicontinuous processing, hemicellulose sugar yield, lignin quality, process intensification

INTRODUCTION

Biorefineries that enable efficient fractionation of sustainable lignocellulosic biomass feeds to its main constituents are central to most biobased value chains and a key technology option for the transition to a circular and biobased society. Over the past decades, organosolv has shown to be an effective treatment for the isolation of cellulose-enriched fibers, hemicellulose sugars and their derivatives (HMF, furfural), and a high purity lignin.⁵⁻⁷ However, a complex operation and relatively high costs and energy demand for solvent recovery have hampered upscaling and market implementation of such processes. 5,8-10

Aqueous acetone organosolv pulping under acidic conditions (the so-called Fabiola process) offers improved performance characteristics in multiple key areas (detailed below), providing a balance between process performance, economics, and sustainability impact. 11 Aqueous acetone is an excellent solvent for lignin, 12 allowing for high biomass

loadings and subsequent lignin concentrations in the liquor with minimal lignin reprecipitation onto the cellulose-enriched pulp. 11 The technology proved excellently scalable from laboratory to the pilot-scale, with the latter using industrialsize wood chips and low liquid-to-solid (L/S) ratios of 3.3 kg 50% aqueous acetone/kg dry wood. 11 Liquid flows were further reduced by replacing the traditional dilutive lignin precipitation approach with the LigniSep process, a continuous lignin precipitation process driven by direct solvent evaporation. Taken together, the volatility of the acetone solvent,⁵ application of low L/S ratios, and continuous lignin

January 11, 2024 Received: Revised: February 7, 2024 Accepted: February 20, 2024 Published: March 1, 2024





precipitation lead to significantly improved process economics and sustainability performance.

The technology also proved highly feedstock tolerant, which helps to mitigate biomass supply risks and to provide an optimal connection to sustainable and economically feasible feedstock supply chains. 13-16 To allow multifeedstock processing, aqueous acetone pre-extraction of complex and mixed biomass streams was introduced as a pretreatment step prior to fractionation to remove organic extractives and minerals. Pre-extraction creates a lignocellulose-enriched stream for improved organosolv processing with high sugar yields and lignin purity as well as valorization potential for the extracted compounds. 17 Such tandem pre-extraction and fractionation does introduce additional processing costs, liquid flows, and energy use, which have to be partly compensated through process intensification as well as optimization of process efficiency (i.e., yield, quality, and value of the biomass fractions).

Fractionation process conditions require one to balance between the high process severity needed to obtain good yields (i.e., solubilized hemicellulose sugars and lignin in the liquor and cellulose enrichment in the pulp) and the mild conditions needed to prevent extensive degradation of these products. 18 In this light, hemicellulose sugar yields still leave room for improvement (currently at ~76%). Improvements in sugar and lignin yield should not come at the expense of lignin quality, though, as a high quality lignin stream is essential for application in, e.g., batteries, ^{19,20} as an antioxidant²¹ or as a polyol for polymer formulations^{22–24} and is as such crucial for the biorefinery viability. 25-27 We recently showed that the Fabiola lignins can be further tailored for specific applications by so-called Partial Depolymerization by Reduction (PDR), a strategy that cleaves residual β -O-4 linkages to reduce the lignin's molar mass and dispersity to yield oligomers better suited for downstream application.^{28,29} PDR efficiency was shown to be directly related to lignin quality, i.e., better results were obtained with less condensed, more β -O-4 ether-rich lignins.²⁸ Sufficient feedstock delignification is needed not only to maximize the isolated lignin yield, but also to yield cellulose pulp of the best quality for material applications³⁰⁻³² or, alternatively, to ensure efficient enzymatic saccharification of the pulp to fermentable monomeric sugars. 5,12 Besides process conditions, delignification is partly dependent on biomass type and the amount of hard-to-extract lignin therein 17,18,33 and was found to vary considerably (72-86%) from feedstock to feedstock. 11,17

In recent years, application development is expanding toward combined use of cellulose fibers, sugar derivatives and/or lignin in composite materials for tailored characteristics, enhanced performance and improved circularity. This further demonstrates the need for biorefineries that enable the isolation of all biomass constituents in high quality.

Improving acetone organosolv fractionation is challenging due to the trade-off between yields and product quality. ^{37,38} Notably, as most hemicellulose and lignin solubilization takes place in the early stages of fractionation, ^{39–41} batchwise processing results in long residence times of solubilized hemicellulose sugars and lignin in the hot liquor, leading to increased degradation of these products.

Karlsson et al. reported a cyclic extraction process consisting of multiple fractionation and pulp washing cycles, thereby reducing the residence time of solubilized lignin at process temperature to less than 5 min, yielding a very high quality lignin. 42,43 A potential drawback, however, may be the increased cost and energy use of processing diluted streams at the biorefinery scale. The advance in lignin quality and color opens opportunities for a high-end application, such as cosmetics, which may compensate for the increased cost and energy use. Zijlstra et al. and Zhou et al. both reported on a flow-through setup for mild organosolv extraction which resulted in improved lignin yield as well as lignin quality as compared to batchwise processing. $^{44-47}$ In addition, both studies used lignin stabilization strategies involving alkoxylation and formylation, respectively, to trap reactive benzylic cations, preserving the lignin β -O-4 bonds and limiting further lignin condensation reactions.

These studies provide support for what may arguably be considered an optimal reactor design for biomass pretreatment: a continuous (screw) reactor with counter-current flow. Indeed, such a process has the potential to improve biorefinery output as well as achieve process intensification through the use of relatively low fractionation L/S ratios and the integration/omission of pulp washing steps. However, the robustness and operational safety of continuous processing may be challenged by continuous transport of (large size) solid biomass particles and a flammable solvent in a pressurized reactor, especially with regard to the abrasion of seals and moving parts. Contrarily, batchwise processing in a percolation reactor has proven to be a robust technology option, as recently reported for acetone organosolv. The envisioned scale-up of this particular process design then consists of an array of such percolation batch reactors, providing a near constant feed for downstream processing.

In this light, we here present a comparison between batchwise processing (Figure 1) and a newly developed

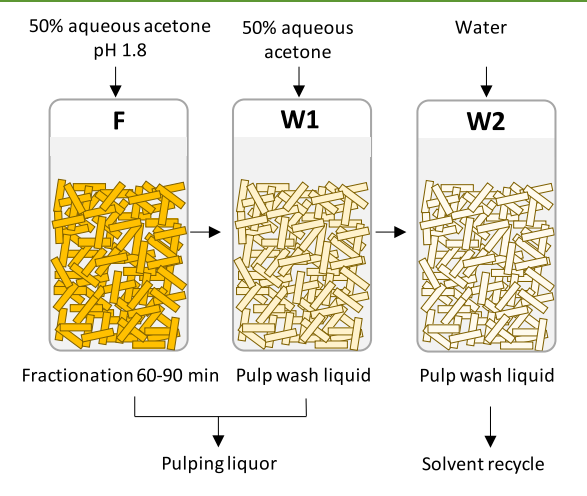
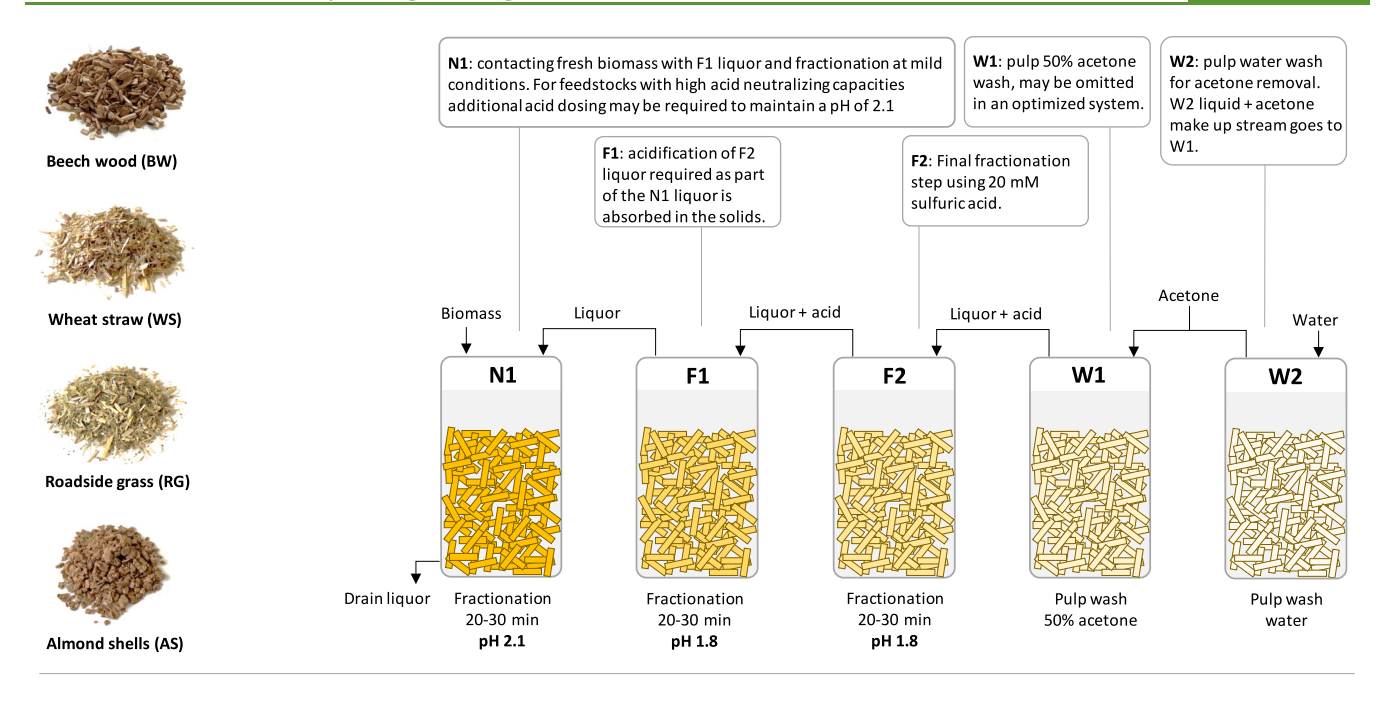


Figure 1. Schematic representation of batchwise processing.

semicontinuous process (SCP) design (Figure 2) based on multistage countercurrent batch extractions reported for, e.g., biomass extraction, mining, and food processing. The SCP process is based on coupling of percolation reactors, allowing for liquor exchange in a stepwise counter-current flow while the biomass solids remain in the reactor. As most of the hemicellulose and lignin are solubilized during the first stages of fractionation, counter-current flow reduces its residence time in the hot liquor, limiting product degradation. We show the potential for improved product yield as well as quality and minimized pulp washing requirements while maintaining the



At the cycle end the solids remain in the reactor, fractionation steps rotate one position counterclockwise (e.g., N1 becomes F1), liquor is transferred two positions counterclockwise (e.g., the new F1 receives the F2 liquor from the previous cycle)

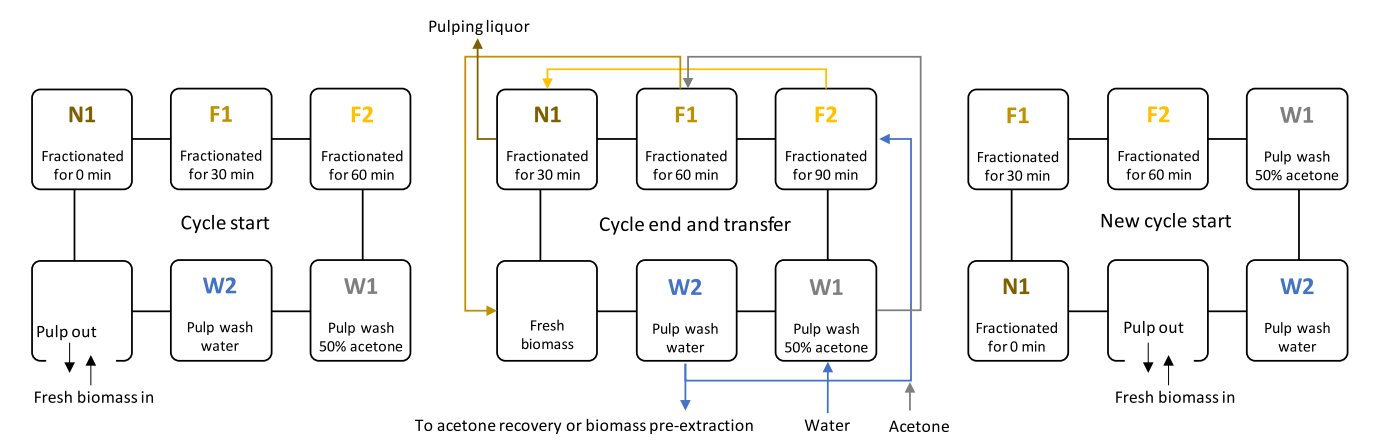


Figure 2. Schematic representation of semicontinuous processing (top), using (eventually, after an initial startup phase) six percolating reactors with fixed solid bed positions and liquid exchange between reactors during the transfer cycle (bottom). See Experimental Section for a detailed process description.

robustness of batchwise operation. The process is explored using beech wood, wheat straw, roadside grass, and almond shells to allow a first assessment of the effects of feedstock type, biomass acid neutralizing capacity, and treated biomass moisture absorbance capacity on process performance.

EXPERIMENTAL SECTION

Feedstocks. Beech wood (BW) with a particle size of 0.75–2 mm was used as received. Wheat straw (WS), roadside grass (RG) were cut to a smaller particle size using a Retsch SM300 cutter mill equipped with a 4 mm sieve. WS, RG, and crushed almond shells (AS, particle size <5 mm) were pre-extracted with water and acetone in a 14 L custom built pre-extraction unit as described for the WA-sequence in previous work. ¹⁷ Biochemical composition analysis was conducted on BW, and the dried pre-extracted RG, WS, and AS are detailed in the Supporting Information, Figure S1 and Table S1.

Semicontinuous Processing Setup. The semicontinuous process design detailed in this study is based on reactor coupling, allowing for liquor exchange between percolation reactors. This way, a stepwise counter-current flow can be achieved while maintaining the

robustness of batchwise operation. The process design is shown in Figure 2 where, in each step, one reactor is emptied and filled with biomass, while the other reactors conduct fractionation and washing steps. Liquid is then transferred counterclockwise after each cycle. Starting from the fresh wash liquid, the individual steps are as follows:

W2. Water is used to remove acetone from the organosolv pulp. The obtained wash liquid contains acetone and is partly transferred to W1 in the following cycle. The remainder is processed for acetone recovery or can be used in the aqueous acetone biomass preextraction process.

W1. Solvent wash of the fractionated pulp using W2 liquid with added acetone (from the solvent recovery) to make a 50% acetone wash liquid

F2. Wash liquid W1 is acidified to pH 1.8 for the final fractionation step of N1/F1 pretreated biomass.

F1. Fractionation of N1 pretreated biomass using transferred F2 liquor.

N1. Fresh prewetted or pre-extracted biomass is contacted with F1 liquor. The aim for N1 is to conduct a mild fractionation (pH 2.1) of the biomass, thereby solubilizing the most labile part of the

Table 1. Experimental Details

						acid added (mM H ₂ SO ₄)			
code	feedstock	process	autoclave	time (min)	L/S ratio (L/kg feed)	B/BR	SCP-F1	SCP-F2	SCP cycles
BW-B	beech wood	batch	20 L	1 * 90	5	40			
BW-BR		batch-reference	2 L	3 * 30	6	40			
BW-SCP		semicontinuous	2 L	3 * 30	6		20	20	2
BW-SCP+		semicontinuous	2 L	3 * 30	6		20	20	4
WS-B	wheat straw	batch	20 L	1 * 60	6	56			
WS-BR		batch-reference	2 L	3 * 20	10	60			
WS-SCP		semicontinuous	2 L	3 * 20	10		30	20	2
RG-B	roadside grass	batch	20 L	1 * 60	6	50			
RG-BR		batch-reference	2 L	3 * 20	10	50			
RG-SCP		semicontinuous	2 L	3 * 20	10		30	20	3
AS-B	almond shells	batch	20 L	1 * 60	6	28			
AS-BR		batch-reference	2 L	3 * 20	10	30			
AS-SCP		semicontinuous	2 L	3 * 20	10		10	20	3

hemicellulose and lignin. After N1, the liquor is drained and processed for lignin and sugar recovery.

After each fractionation cycle, the liquid is drained and transferred while the solids remain in the reactor. Note that part of the liquid is absorbed in the solids and is thus not transferrable. As a result, the liquid in each fractionation and washing step consists of both the transferred liquid and the absorbed liquid from the previous cycle. In Figure 2 the fractionation cycles and liquor transfer scheme is presented where fractionation stages move one position counterclockwise in each cycle. For example, the bottom left reactor in the cycling scheme of Figure 2 is loaded with biomass, which then undergoes 3 fractionation cycles (N1, F1, and F2) followed by 2 washing cycles (W1 and W2). The solids remain the bottom left reactor during these cycles and are removed during the sixth cycle. While the fractionation and wash steps move one position counterclockwise after each cycle, the transferrable liquid moves two positions counterclockwise (e.g., F1 liquor to the fresh biomass to start the N1 step in the next cycle). Note that despite the apparent complexity, the system is not very different from the series of parallel percolation reactors anticipated for a larger-scale biorefinery operation.

Small Scale Screening Experiments. A series of screening experiments were conducted to determine the correlation between liquor acidity and fractionation performance, furfural formation, and stability, as well as the effect of biomass acid neutralizing capacity (ANC) on liquor pH and fractionation performance. Methodology and results are available in the Supporting Information. Additional experiments were conducted to obtain lignins with varying quality. In an ASE350, beech wood was fractionated at 140 °C using 50% acetone (5 L/kg dry wood) and 40 mM H₂SO₄. After 15 min of fractionation time, the liquor was replaced with fresh reaction liquid and the fractionation continued for another 15 min. In total, the beech wood was fractionated six times for 15 min to a total reaction time of 90 min. Lignin was isolated from the combined liquors, yielding the B15 lignin sample. Similarly, the experiment was repeated using fresh beech wood and three fractionation runs of 30 min, two runs of 60 min, and one run of 120 min, yielding the B30, B60, and B120 lignins. Note that lignin concentrations in the liquor vary per experiment and concentration effects on, for example, condensation reactions are not accounted for.

Batchwise Processing Experiments. The results of previously published work were used as basis for comparison between batchwise processing and SCP; beech wood (here BW-B, previously L-BEC), ¹¹ pre-extracted wheat straw (here WS-B, previously WA-WS), ¹⁷ pre-extracted roadside grass (here RG-B, previously WA-RG), ¹⁷ and pre-extracted almond shells (here AS-B, previously WA-AS) ¹⁷ were processed in a 20 L reactor using the process conditions, as shown in Table 1.

Semicontinuous Processing Experiments. The experiments were conducted using a single 2 L reactor, where the reaction mixture

was heated to 140 $^{\circ}$ C and kept isothermal for the defined reaction time. After the reactor was cooled, the reaction liquid was obtained by pumping liquor out of the reactor. The obtained solids and liquids were then used for the next SCP cycle. In total, 12–18 fractionation runs were conducted to simulate a single SCP experiment (Figures S6 and S7). The initial experimental design aimed to fractionate all feedstocks using a L/S ratio of 6 L/kg dry feedstock, mostly in line with the published results from batchwise processing. However, the high liquid absorption capacity of WS and RG prevented reasonable liquid transfer at this L/S ratio, and therefore, WS and RG, as well as AS, experiments were done using a higher L/S ratio of 10 L/kg dry feedstock.

Active pH control was not available for the experiments. Therefore, $20\,$ mM $\,H_2SO_4$ was used for the acidification of the F2 liquid. Additional acid was used to lower the pH for the F1 fractionation step to maximize fractionation and to better cope with the ANC of the fresh biomass during the N1 step in the next cycle. Except for wheat straw, the overall acid concentrations in the F1 step were kept identical to the batch reference experiments.

The washing steps W1 and W2 were not included in the SCP liquid transfer, but were conducted and analyzed separately to limit the experimental complexity. An additional test was conducted for BW-SCP, where improved liquid transfer (BW-SCP+) was tested by incorporation of the W1 wash liquid in the liquid transfer scheme (Figure S7). Fully detailed experimental procedures and methodology are available in the SI.

Batchwise Reference Processing Experiments. To enable a more accurate comparison between batchwise processing and SCP, an additional reference experiment (-BR) was conducted for each

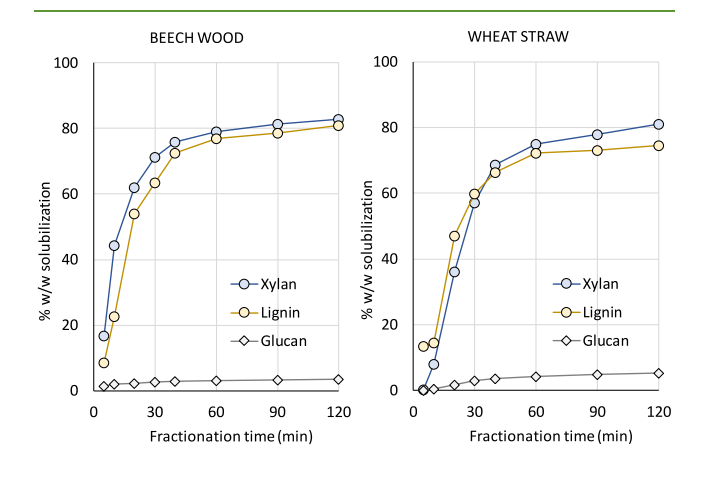


Figure 3. Development of beech wood and wheat straw fractionation at 140 °C over time using 50% aqueous acetone and 20 mM H₂SO₄.

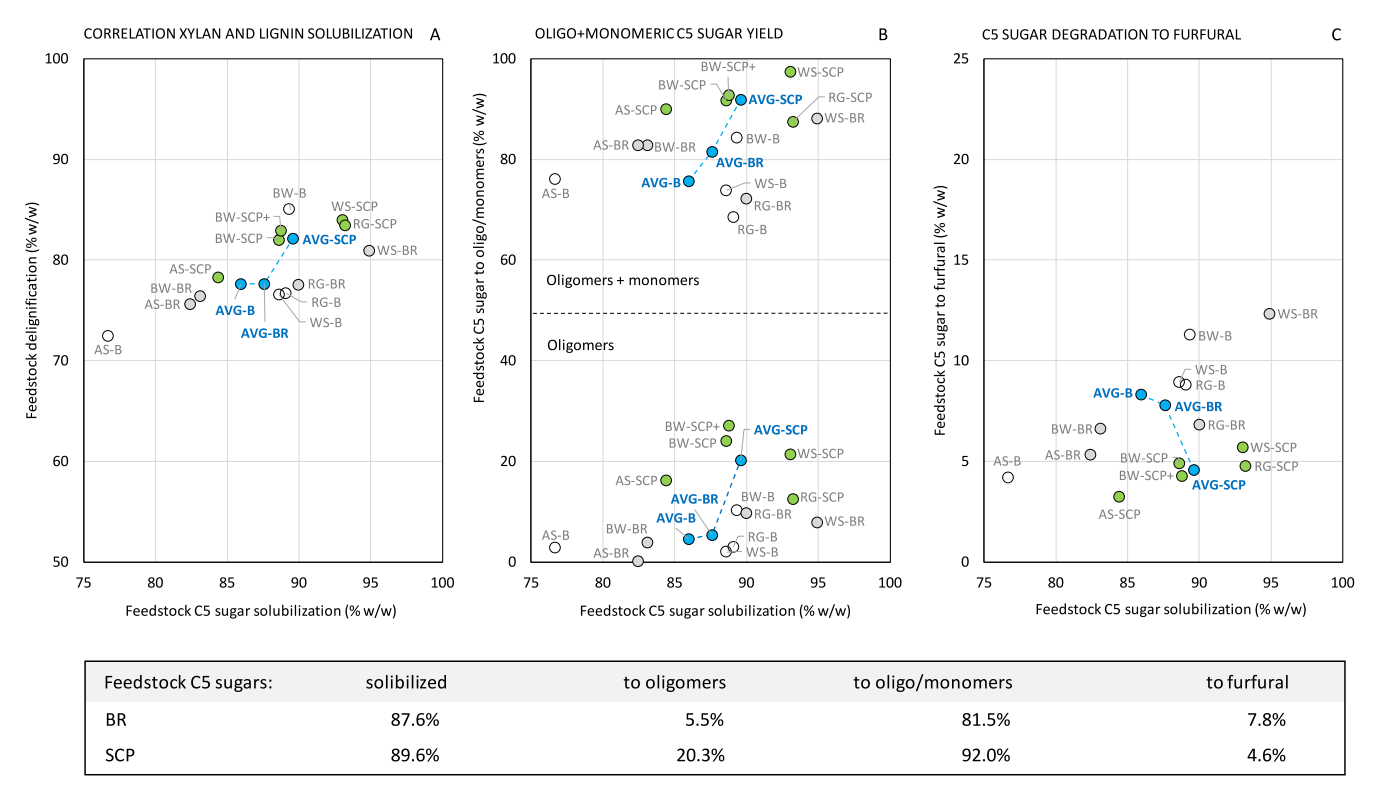


Figure 4. Batchwise (B, open circles), batchwise reference (BR, gray circles), and semicontinuous processing (SCP, green circles) of beech wood, wheat straw, roadside grass, and almond shells. Correlation between feedstock polymeric C5 sugar solubilization and delignification (A), conversion of feedstock C5 sugars to oligo and monomeric sugars (B) and conversion of feedstock C5 sugars to furfural (C). The table at the bottom shows the average yields (BW, WS, RG, AS) of oligomers, oligomers + monomers, and furfural.

feedstock using identical scale, heating/cooling cycles, and L/S ratios as applied for SCP. The 2 L and 20 L reactor heating curves and definitions of the reaction times are available in the SI, Figure S9.

RESULTS AND DISCUSSION

Batchwise vs Semicontinuous Fractionation: Fate of the Hemicellulose. BW and WS were fractionated batchwise using liquor replacement by fresh reaction liquid (50% acetone, 20 mM H₂SO₄) at selected times, as shown in Figure 3. As expected, fractionation proceeds fast in the early stages of the process, with the initial WS fractionation being slightly slower than BW, as the higher ANC of the straw must be overcome first. Depending on the acid concentration, most hemicellulose sugars (xylan, arabinan, galactan, mannan, and rhamnan) are solubilized in the first 20-30 min of fractionation (Figures S2 and S3). Solubilization of glucan is limited and likely originates from hydrolysis of the amorphous cellulose regions. The early release of (oligomeric) sugars during batchwise processing results in a relatively long residence time of these sugars in the acidic liquor, leading to increased sugar degradation (Figure S4). Overall, the rapid solubilization of the hemicellulose sugars (and lignin, see below) in Figure 3 indeed suggests that a process design with counter-current flow is warranted to minimize the average residence time of these solubilized products in the hot liquor.

The hemicellulose mass balances for batch (-B), batch-reference (-BR), and semicontinuous processing (-SCP) in this study are restricted to the C5 sugars component (xylan and arabinan) only as these sugars represent on average 93% of the hemicellulose sugars in the selected feedstocks, and both xylose and arabinose degrade to furfural. Oligomeric and monomeric C5 sugar yield and degradation, as well as lignin characteristics,

are affected not only by process design (batch vs semi-continuous), but also by variations in liquor acidity. In the absence of an inline pH control system, estimation of the required acid dose to reach the defined target pH is complicated by the combined effect of the applied L/S ratio, variations in biomass ANC and, in the case of SCP, the efficiency of liquid transfer. As a result, the liquor pH shows some variation (Figure 9F) that will impact fractionation performance. Therefore, the fractionation results in Figure 4 are plotted as a function of C5 sugar solubilization, which is taken as a measure for process severity, allowing for more accurate comparison between the experiments.

In Figure 4A, the extent of feedstock C5 sugar solubilization correlates well with feedstock delignification. Batchwise fractionations with high delignification and sugar solubilization (e.g., BW-B, pulping liquor pH 1.6) furthermore showed increased C5 sugar degradation to furfural (Figure 4C). Conversely, the milder fractionations with less delignification and sugar solubilization (e.g., AS-B, pulping liquor pH 1.8) lead to less furfural formation. Note that, besides liquor acidity, feedstock type and characteristics may also determine fractionation performance as shown by the herbaceous biomass types WS-B and RG-B, which perform better than AS-B at identical pulping liquor acidity.

Overall, slightly improved fractionation performance is observed for the BR experiments compared to B, indicating some effect of the repeated heating/cooling cycles applied in a 2 L reactor for BR as compared to the single fractionation run in a 20 L reactor for the B run. Here, BW-BR and AS-BR have more similar pulping liquor acidities (i.e., 1.8 and 1.7, respectively) resulting in a comparable fractionation performance.

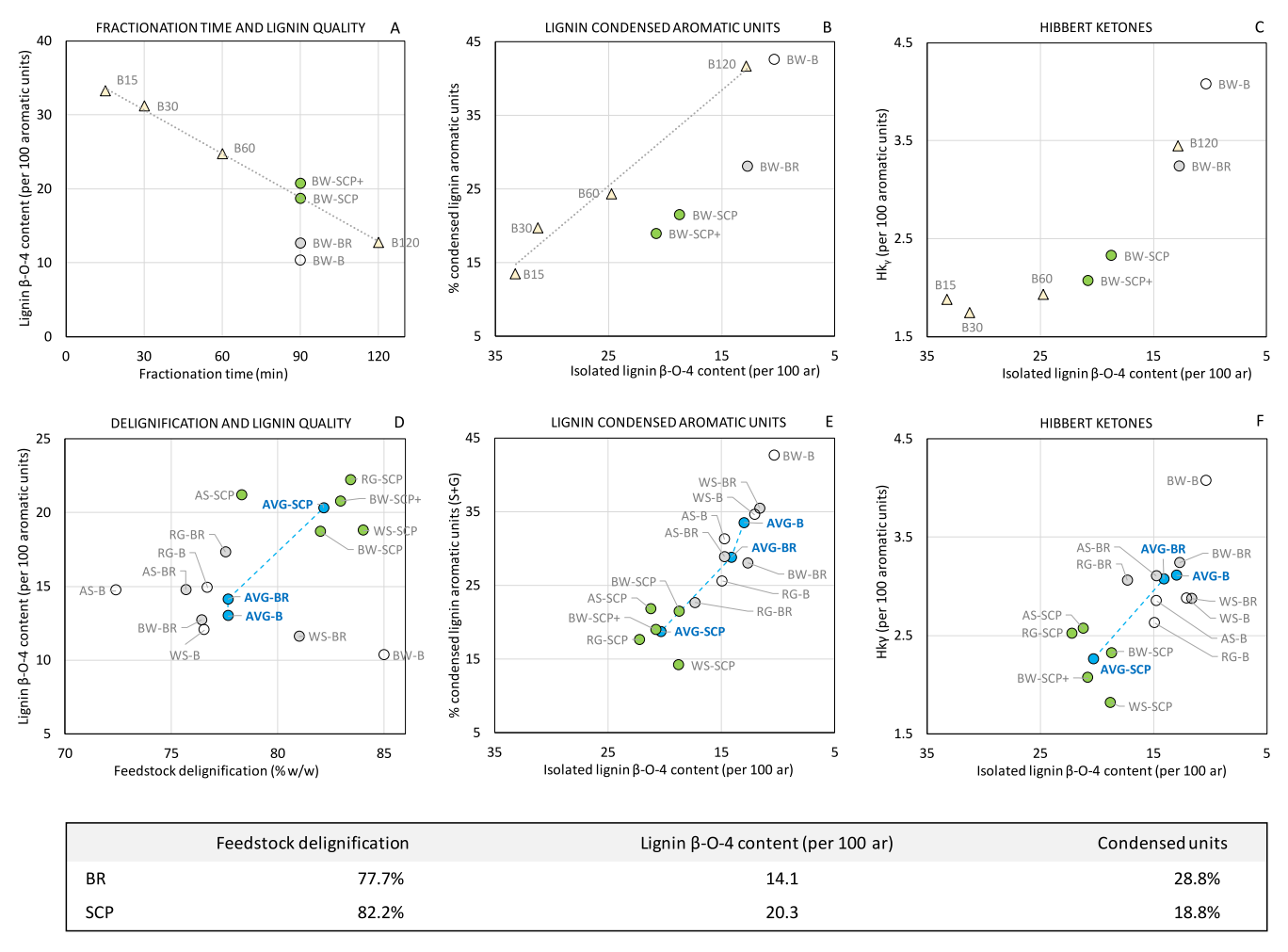


Figure 5. Fractionation time series (yellow triangles) of beech wood and batchwise (B, open circles), batchwise reference (BR, gray circles), and semicontinuous processing (SCP, green circles) of beech wood, wheat straw, roadside grass, and almond shells. Correlation between fractionation time and lignin quality (A), delignification and lignin quality (D), isolated lignin β-O-4 content and abundance of lignin condensed aromatic units (B, E) and isolated lignin β-O-4 content and abundance of Hibbert ketones (C, F). The table at the bottom shows the average yields (BW, WS, RG, AS) for delignification and lignin quality.

SCP further improved C5 sugar and lignin removal from the feedstock as compared to the B and BR experiments. Besides enhanced fractionation, the counter-current flow may provide better separation of the solubilized products from the cellulose enriched pulp, limiting lignin reprecipitation onto the pulp fibers during the W2 water wash. 11,54 Excitingly and contrary to batchwise processing, the enhanced fractionation observed for SCP is combined with reduced furfural formation, showing an important decoupling of applied process severity (i.e., sugar solubilization) and sugar degradation. In addition, the presence of oligomeric C5 sugars in the SCP liquors increased 4-fold (on average 20% of feedstock polymeric C5 sugars) as compared to the B and BR runs. As expected, the oligomers mostly originated from the N1 fractionation step (Figures S11 and S16). The oligomers may still contain acetyl groups, as the total acetic acid yield is lower for the SCP as compared to the B and BW experiments (Figure S15). The more complex BW-SCP+ experiment, which aimed at reduction of the amount of liquor absorbed in the biomass solids after draining and thus improved counter-current flow (see Figure S8 for the methodology), resulted in a minor improvement in sugar yield as compared to BW-SCP.

Batchwise vs Semicontinuous Fractionation: Fate of the Lignin. Contrary to sugar chemistry, lignin structural changes during fractionation are complex. Lignin solubilization occurs via (acid-catalyzed) cleavage of lignin β -O-4 linkages which starts with elimination of the α -hydroxyl group of the linkage generating a reactive carbenium ion and, depending on the pathway, a Hibbert ketone end group. Both of which are involved in lignin repolymerization/condensation reactions and formation of stabile C–C bonds.

To provide better insight into the gradual changes that occur in the (solvated) lignin structures during fractionation, additional experiments with varying fractionation times were conducted using beech wood. For the B15 experiment, the solvent was replaced with fresh reaction liquid every 15 min to a total reaction time of 90 min, after which the lignin was isolated from the combined liquor from the 6 cycles. Similarly, the experiment was repeated using fresh beech wood and three fractionation runs of 30 min, two runs of 60 min, and one run of 120 min, yielding the B30, B60, and B120 lignins. This way, lignin samples were obtained with varying residence times in the hot liquor, but keeping the total processing time constant. As a result, beech wood delignification was constant at \sim 80–84%, the same as that for batchwise processing. The β -O-4

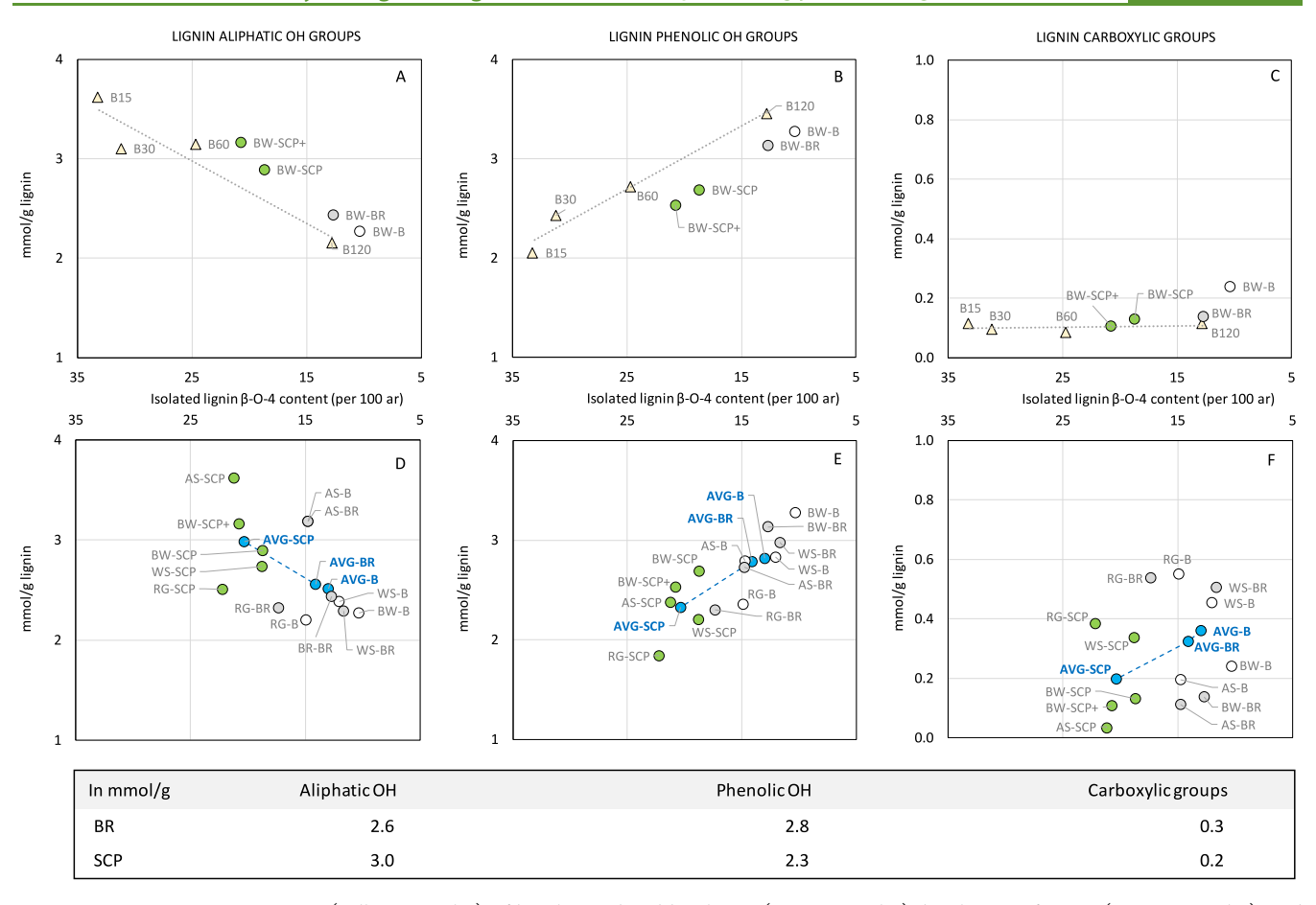


Figure 6. Fractionation time series (yellow triangles) of beech wood and batchwise (B, open circles), batchwise reference (BR, gray circles), and semicontinuous processing (SCP, green circles) of beech wood, wheat straw, roadside grass, and almond shells. Correlation of isolated lignin β-O-4 content and isolated lignin aliphatic hydroxyl groups (A, D), phenolic hydroxyl groups (B, E), and carboxylic groups (C, F). The table at the bottom shows the average abundance (BW, WS, RG, AS) of lignin hydroxyl groups.

content of the native lignin in the BW and WS feedstocks were previously quantified to be 53 and 41 per 100 aromatic units, respectively. 17,28

All isolated lignins were characterized using 2D-HSQC NMR analysis to assess the extent of lignin β -O-4 bond cleavage, depolymerization (formation of Hibbert ketone end groups), and repolymerization (condensation). 2D-HSQC NMR spectra and quantification of major structures and linkages are available in the Supporting Information (Figures S20-S25 and Tables S6 and S7). Figure 5A-C shows the beech wood lignins only to provide support for assessment of the B, BR, and SCP lignin characteristics in Figure 5D-F. In Figure 5A, the lignin β -O-4 content, plotted as a function of reaction time, shows a linear decrease. The β -O-4 content of the BW-B and BW-BR lignins (10.3 and 12.7, respectively) does not correlate exactly with the B15-120 lignins, possibly due to differences in equipment, reactor volume, heating rates, etc. Excitingly, BW-SCP and BW-SCP+ show a marked improvement in lignin β -O-4 content compared to the B and BR experiments in similar experimental equipment (with equal heating/cooling rate) with 18.7 and 20.8 linkages per 100 aromatic units, respectively.

In Figure 5D, the β -O-4 content of all B, BR, and SCP lignins are related to the feedstock delignification to include a measure for process severity. Despite some (feedstock-related) variation, the SCP clearly shows improved delignification, and the isolated lignins have a higher β -O-4 content as well as a

lighter color (Figure 9) as compared to the B and BR lignins. The stepwise counter-current flow approach thus combines an improved C5 sugar mass balance with an improved lignin product yield and quality.

Another way of relating process design and severity to lignin characteristics is to correlate structural characteristics with the lignin β -O-4 content. Figure 5B, for example, shows the extent of lignin condensation as a function of β -O-4 content (see also Figure S17 for methodology). As expected, the B15–120 series show an increased presence of condensed syringyl and guaiacyl units in the lignins with lower β -O-4 content. The B, BR, and SCP lignins of BW show a similar trend, although being less condensed than the B15–120 lignins.

The compiled data of all feedstock lignins in Figure 5D–F further follow the BW correlations, with the SCP lignins showing more β -O-4 bonds, less condensation, and less Hibbert ketone end groups. These results are in line with those reported in studies using flow reactors.^{44,57}

Typically, lignin β -O-4 bond cleavage leads to the loss of primary aliphatic OH groups and the liberation of phenolic OH groups. ⁵⁸ Figure 6 A and B clearly show the expected correlation for the B15–120 lignins in terms of higher aliphatic OH retention at higher β -O-4 bond content. Notably, the aliphatic OH content of BW-SCP and BW-SCP+ lignins is relatively high. Interference from sugar signals in the assigned region for aliphatic hydroxyl in the ³¹P NMR spectra does not seem to be a major contributor as the sugar content of the

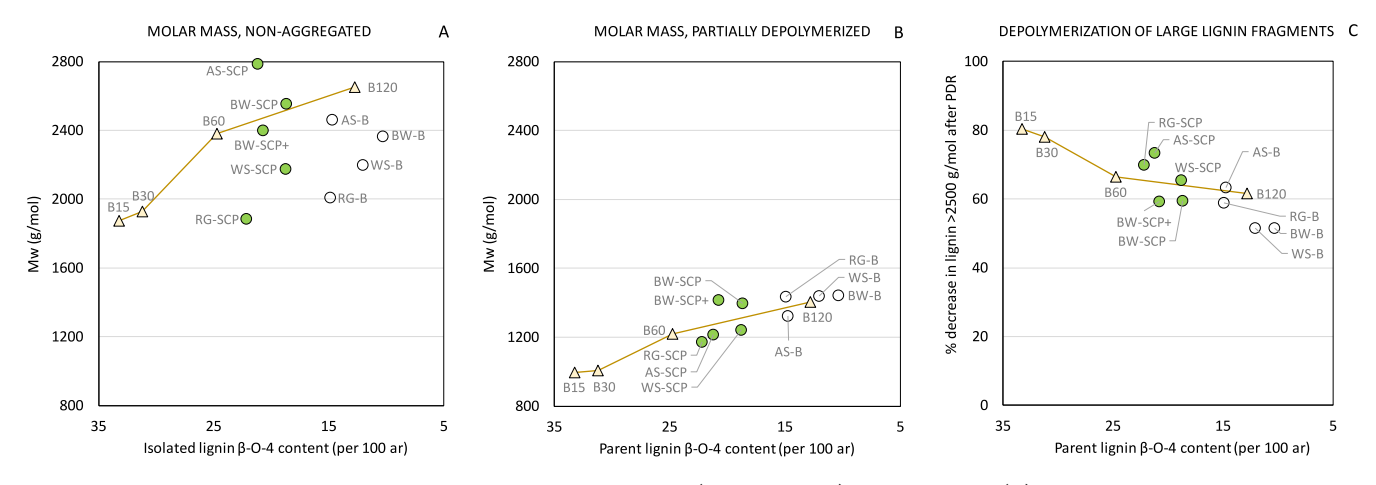


Figure 7. Correlation between isolated lignin β -O-4 content and $M_{\rm w}$ of (nonaggregated) isolated lignins (A) and partially depolymerized lignins (B) and the extent of depolymerization of large lignin fragments (C).

isolated lignins is relatively low (Figure S18). ⁵⁹ In addition, a range of lignin carbohydrate assignments ⁶⁰ (benzyl ethers, phenyl glycosides, and γ -esters) in the 2D-HSQC NMR spectra of the isolated lignin did not reveal significant presence of Lignin Carbohydrate Complexes (LCC). Note that LCC may be present in the hemicellulose hydrolysate (obtained after lignin isolation), as reported by Narron et al. ⁶¹ In our study, lignin precipitation yield is generally below 100%, indicating the presence of LCC in the hemicellulose hydrolysates. However, some (feedstock related) variation hampers correlation between treatments, and a more in depth study is needed for quantification, characterization, and isolation of LCC.

Feedstock origin strongly determines the hydroxyl group content of the isolated organosolv lignins, ⁶² and indeed, a significant variation in aliphatic, phenolic, and carboxylic hydroxyl group content is observed, Figure 6D–F. However, each specific feedstock shows similar trends with more aliphatic OH and less phenolic and carboxylic OH groups for the SCP lignins, as compared to the B and BR lignins.

The molar mass of lignin is affected by depolymerization and recondensation reactions, generally depending on temperature, time and liquor acidity. 56 As detailed in previous work, lignin aggregates can cause an overestimation of lignin molar mass when alkaline Size Exclusion Chromatography is used for the analysis. Therefore, the weight average molecular weight (M_w) in Figure 7 shows the lignin $M_{\rm w}$ analyzed after a deaggregation treatment at 150 °C in methanol (see also Figure S19 and Tables S6 and S7). The B15-120 lignin $M_{\rm w}$ in Figure 7A shows a significant increase in molar mass over a decreasing lignin β -O-4 bond content. More extensive cleavage of lignin β -O-4 bonds may initially yield smaller lignin fragments but this is likely more than offset by increased condensation reactions, as shown in Figure 5B. As seen previously,²⁸ the effectiveness of the lignin PDR process in producing a lower molar mass lignin again correlates strongly with the presence of cleavable β -O-4 linkages vs noncleavable C–C bonds that form upon lignin condensation. The B15-120 lignins were subjected to PDR (10 g/L lignin in methanol, 120 min, 0.5 g Ru/C per g lignin, 20 bar H_2) and the resulting lignin M_w is shown in Figure 7B. The PDR process aims to depolymerize the large lignin fragments, which are relatively rich in β -O-4 bonds, to enrich the sample in lignin oligomers with lower molar mass and dispersity. As done previously, 28 we arbitrarily

set the cutoff for large lignin fragments at to >2500 g/mol and expressed these as a percent of the total lignin SEC signal. The large lignin fragments in the B15 lignin contributed to 15% of the total SEC signal which decreased to 3% after PDR, showing effective depolymerization. The more condensed B120 lignin contained more large lignin fragments before and after PDR with 23% and 9%, respectively. The percent decrease in lignin >2500 g/mol after PDR is presented in Figure 7C showing more effective depolymerization for the less-condensed lignins. Significant variation in $M_{\rm w}$ is observed for all B and SCP lignins, with a relatively large spread between feedstock types. PDR treatment, however, significantly reduces both the $M_{\rm w}$, dispersity, and feedstock related molar mass variation with the SCP lignins showing slightly improved depolymerization, in line with the B15–120 trend. Similarly,

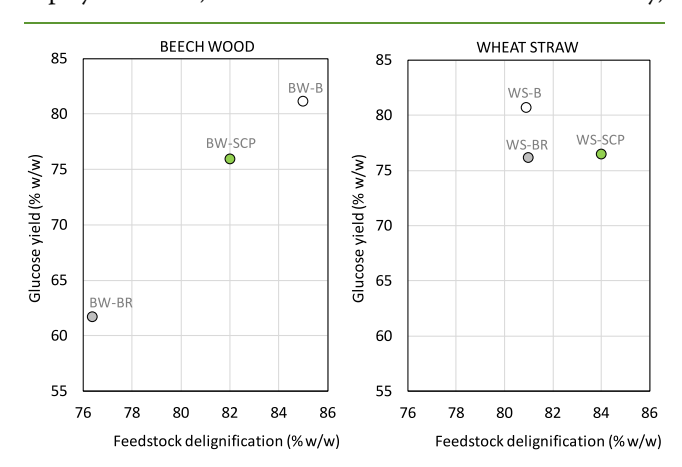


Figure 8. Enzymatic saccharification of pulps; correlation glucose yield and feedstock delignification of BW and WS pulps.

the depolymerization of large lignin fragments is more effective for the SCP lignins as compared to the B ones. Note that high lignin concentrations during PDR and a lower PDR temperature may reveal larger differences between lignins from B and SCP. Overall, the results show there is still quite some upward potential for SCP lignin quality and susceptibility to partial depolymerization, as indicated by the B15 and B30 lignins.

Batchwise vs Semicontinuous Fractionation: Fate of the Cellulose. Cellulose (glucan) enrichment in the obtained pulps from SCP is slightly higher as compared to B and BR

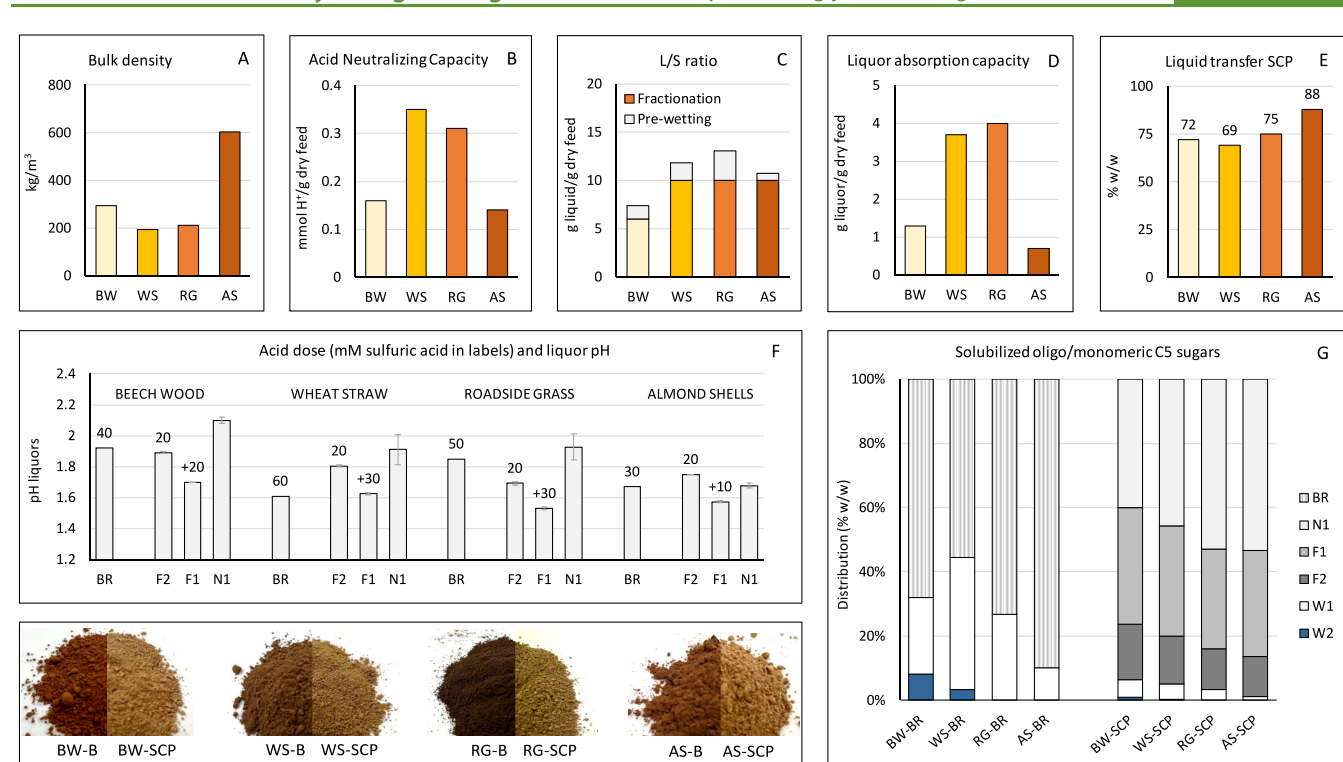


Figure 9. Bulk density of feedstocks (A), acid neutralizing capacity of feedstocks (B), applied liquid-to-solid ratio for biomass prewetting and fractionation (C), liquor absorption capacity of feedstocks (D), average liquid transfer during SCP (E), pH of SCP and BR liquors with the applied and added sulfuric acid concentration in mM (F), and distribution of the total recovered oligomeric and monomeric C5 sugars over BR and SCP liquors (G). BW, WS, RG, and AS lignins isolated after batchwise (left) and the lighter colored lignin isolated after semicontinuous processing (right) are shown at the bottom.

AS-B

AS-SCP

pulps as a result of improved hemicellulose and lignin removal during SCP (Table S3 and Figure S13). However, pulp composition is mostly determined by feedstock origin, composition, content of fractionation-recalcitrant hemicellulose/lignin, and applied process severity.

WS-B

RG-B

RG-SCP

Optimization of SCP toward further improved delignification by increasing process severity during the F2 fractionation step may benefit both pulp material applications as well as the enzymatic saccharification of pulp glucan to glucose for subsequent fermentation to fuels and chemicals. Notably, a strong correlation was found between BW delignification (i.e., pulp residual lignin content) and glucose yield after enzymatic saccharification using enzyme solution MetZyme SUNO 036 from Metgen and an enzyme dose of 0.15 g enzyme mixture/g pulp glucan (for yields see Figure 8). Surprisingly, the correlation was not found for the WS pulp.

Process Considerations. Process severity is one of the main factors controlling the fractionation performance as well as the product yield and quality. Tuning of the process severity for the aqueous acetone process is mostly achieved through liquor acidification. As shown in Figure 9F, an acid concentration of 20 mM H₂SO₄ is sufficient to come close to pH 1.8 in the F2 pulping liquor, regardless of feedstock type. The liquor pH of the F1 step is affected by the solids and absorbed liquor therein coming from N1, which has a target pH of 2.1. Consecutively, the N1 step is affected by the acidity of the transferred F1 liquor and biomass ANC (Figure 9B). Feedstock flexibility and processing of complex and mixed streams of lignocellulosic biomass are a priority for aqueous acetone organosolv process development. To cope with the inherent differences in biomass ANC, active pH control must

be implemented in a scaled-up design. Besides stable processing under predefined severities, pH control also allows for optimization of each SCP step regarding product yield and quality.

Further tuning of the N1 step and balancing product yield and quality are important for further SCP development. In addition, optimization of N1 enables the use of biomass ANC to reduce process acid and lime requirements, adding sustainability advancement to the process. Despite being below the pH 2.1 target, the SCP liquors are less acidic than the ones obtained from B and BR. As a result, the obtained hydrolysates after acetone recovery and lignin precipitation need on average 25% less Ca(OH)₂ to neutralize to pH 7 (Table S8).

A more challenging aspect for further SCP development pertains to liquid flows. Viable biorefinery economics require low L/S ratios for fractionation and efficient pulp washing to minimize liquid flows and the energy demand for solvent recovery. At the lab-scale, previously reported batchwise fractionations were conducted using a relatively low L/S ratio of 5-6 L/kg of dry feedstock (excluding an additional L/ S ratio of 3 for pulp washing liquor), similar to the BW-SCP fractionation reported here. However, it was found that the high liquid absorption capacity of WS prevented reasonable liquid transfer at L/S 6 and therefore WS as well as RG and AS experiments were done using a higher L/S ratio of 10 L/kg dry feedstock (Figure 9C,D). Overall, the sum of liquid needed for batch fractionation and subsequent pulp washing is quite similar to SCP where the washing liquid can be integrated into the counter-current flow. For optimal alignment with a SCP design including biomass pre-extraction where a wet extracted

biomass is transferred to the fractionation step, all feeds were prewetted using 50% aqueous acetone. This step was also needed to ensure sufficient liquid transfer after N1. Prewetting increased the fractionation L/S ratio to 7, 12, 13, and 11 L/kg dry BW, WS, RG, and AS, respectively.

Efficient liquid transfer between SCP cycles is crucial to minimizing sugar and lignin degradation and is largely controlled by the biomass liquor absorption capacity. Unfortunately, the absorption capacity does not decrease significantly upon fractionation, and similar capacities were found in the final cellulose-enriched pulps (except for RG, data not shown). WS had the highest absorption capacity throughout processing as evidenced by the liquid transfer of 69% w/w in Figure 9D. Contrarily, the high bulk density and low liquor absorption capacity of AS resulted in the most efficient liquid transfer of 88%. In Figure 9G the total amount of isolated C5 sugars (oligomers and monomers) from the pulping liquor and W1 and W2 wash liquors is set to 100%, showing the distribution of these sugars over the liquids. The isolated lignin shows a similar distribution, except for W2 liquids, where the acetone content was too low for lignin solubilization. Retention of sugars in the pulp after BR is in line with the applied L/S ratios and feedstock liquor absorption capacities (e.g., highest retention for WS, lowest for AS). For the SCP experiments in Figure 9G, the percentage of product found in the N1 liquor comprises the total of the gray bars (N1 + F1 + F2) with a further differentiation of sugars found in the F2 and F1 liquors, showing how much of the sugars were transferred in each step.

On average, stepwise counter-current flow during SCP increased the product recovery in the liquor from 73% for BR to 97% for SCP. Future integration of W1 pulp wash in the SCP cycles will maximize product recovery in the pulping liquor. Exploratory pulp water wash experiments show that depending on feedstock particle size, a significant part of the (first) water wash liquid can be used for transfer to the W1 step (Figure S26). Overall, this shows potential for minimizing the use of washing liquids and dilution of pulping liquors with W1 wash liquor.

CONCLUSIONS

The robustness of batchwise processing with, for example, percolation reactors is an important prerequisite for further scale-up of the acetone organosolv process. Modification of an array of parallel reactors to allow liquid transfer between reactors in a stepwise counter-current operation is now shown to combine this robustness with an opportunity for process intensification and for improvements in yield and quality of the biorefinery output.

A first exploration demonstrates that semicontinuous processing indeed has the potential to improve fractionation performance. More C5 sugars were solubilized from the biomass, and less sugars degraded to furfural, leading to improved C5 (oligo or monomeric) sugar yields of 92% (up from 82%). The increase in the production of (potentially acetylated) oligomeric C5 sugars in SCP requires careful consideration as to how this may impact the biorefinery output. Oligomer characteristics and the cost-effectiveness of its isolation and purification will largely determine the valorization potential of this product stream. Importantly, SCP improved both feedstock delignification and lignin quality. The isolated lignin is lighter in color and contains more β -O-4 bonds and aliphatic hydroxyl groups. The more

native nature of the lignin resulted in improved partial depolymerization to more reactive lignin building blocks with lower molar mass and dispersity. The depolymerized lignins may be used in a range of biobased polymer applications with a high lignin content and tunable characteristics.

Furthermore, SCP may provide an advantage in terms of process intensification and improved process economy by integrating the pulp washing (and optionally biomass pre-extraction) steps. Further development and fine-tuning of SCP may bring additional sustainability impact from reduced acid and lime use as compared to batchwise processing.

This study clearly demonstrates the benefits of SCP for a selection of different feedstocks. However, feedstock-specific differences in performance are observed, which need careful consideration. The first relates to active pH control using inline pH measurement and an acid dosage system to ensure mild fractionation conditions during the N1 step and more acidic conditions in the following steps, despite differences in biomass ANC. Such electrodes have now been tested at the lab-scale, providing the potential for implementation into SCP. The second aspect relates to conflicting needs regarding liquid use. On the one hand, enough liquid is needed to ensure efficient liquor transfer between SCP steps, especially for feedstocks with a high liquor absorbance capacity. On the other hand, low liquid usage is imperative for maintaining a positive biorefinery economy and sustainability impact. After this first proof-of-concept, further development is required by using customized connected reactors. The main emphasis is then on inline pH control and liquor transfer, as these aspects directly impact process performance as well as product quality.

ASSOCIATED CONTENT

Supporting Information

The Supporting Information is available free of charge at https://pubs.acs.org/doi/10.1021/acssuschemeng.4c00303.

Additional experimental details, materials, methods, results, and 2D-HSQC NMR spectra (PDF)

AUTHOR INFORMATION

Corresponding Author

Arjan T. Smit — The Netherlands Organisation for Applied Scientific Research (TNO), Energy and Materials Transition, Biobased and Circular Technologies Group, 1755 ZG Petten, The Netherlands; Organic Chemistry and Catalysis, Institute for Sustainable and Circular Chemistry, Utrecht University, 3584 CG Utrecht, The Netherlands; orcid.org/0000-0002-8685-3850; Email: arjan.smit@tno.nl

Authors

Michiel Hoek – The Netherlands Organisation for Applied Scientific Research (TNO), Energy and Materials Transition, Biobased and Circular Technologies Group, 1755 ZG Petten, The Netherlands

Petra A. Bonouvrie – The Netherlands Organisation for Applied Scientific Research (TNO), Energy and Materials Transition, Biobased and Circular Technologies Group, 1755 ZG Petten, The Netherlands

André van Zomeren – The Netherlands Organisation for Applied Scientific Research (TNO), Energy and Materials Transition, Biobased and Circular Technologies Group, 1755 ZG Petten, The Netherlands; orcid.org/0000-0002-0670-4100

- Luke A. Riddell Organic Chemistry and Catalysis, Institute for Sustainable and Circular Chemistry, Utrecht University, 3584 CG Utrecht, The Netherlands
- Pieter C. A. Bruijnincx Organic Chemistry and Catalysis, Institute for Sustainable and Circular Chemistry, Utrecht University, 3584 CG Utrecht, The Netherlands; © orcid.org/0000-0001-8134-0530

Complete contact information is available at: https://pubs.acs.org/10.1021/acssuschemeng.4c00303

Author Contributions

The manuscript was written through contributions of all authors. All authors have given approval to the final version of the manuscript.

Notes

The authors declare no competing financial interest.

ACKNOWLEDGMENTS

This project has received TNO funding from the Dutch Ministry of Economic affairs. We thank the NMR group at Utrecht University for the access to their facilities. We are grateful to the following persons for their excellent contribution to this work: Karina Vogelpoel-de Wit, Ben van Egmond, Thomas Klijbroek, Esther Cobussen-Pool, Thomas Dezaire, Kasper Tempel, Patrick Kreft, and Laura Rozing.

REFERENCES

- (1) Kumar, B.; Bhardwaj, N.; Agrawal, K.; Chaturvedi, V.; Verma, P. Current perspective on pretreatment technologies using lignocellulosic biomass: An emerging biorefinery concept. *Fuel Process. Technol.* **2020**, *199*, 106244.
- (2) Ragauskas, A. J.; Beckham, G. T.; Biddy, M. J.; Chandra, R.; Chen, F.; Davis, M. F.; Davison, B. H.; Dixon, R. A.; Gilna, P.; Keller, M.; et al. Lignin valorization: improving lignin processing in the biorefinery. *Science* **2014**, *344* (6185), 1246843.
- (3) Sharma, V.; Tsai, M.-L.; Nargotra, P.; Chen, C.-W.; Sun, P.-P.; Singhania, R. R.; Patel, A. K.; Dong, C.-D. Journey of lignin from a roadblock to bridge for lignocellulose biorefineries: A comprehensive review. *Sci. Total Environ.* **2023**, *861*, 160560.
- (4) Sridevi, V.; Suriapparao, D. V.; Tanneru, H. K.; Prasad, K. An Overview on Organosolv Production of Bio-refinery Process Streams for the Production of Biobased Chemicals. *Thermochemical and Catalytic Conversion Technologies for Future Biorefineries*; Springer, 2022; Vol. 1, pp 345–374.
- (5) Zhang, Z.; Harrison, M. D.; Rackemann, D. W.; Doherty, W. O.; O'Hara, I. M. Organosolv pretreatment of plant biomass for enhanced enzymatic saccharification. *Green Chem.* **2016**, *18* (2), 360–381.
- (6) Wei Kit Chin, D.; Lim, S.; Pang, Y. L.; Lam, M. K. Fundamental review of organosolv pretreatment and its challenges in emerging consolidated bioprocessing. *Biofuel. Bioprod. Biorefin.* **2020**, *14* (4), 808–829.
- (7) Salapa, I.; Katsimpouras, C.; Topakas, E.; Sidiras, D. Organosolv pretreatment of wheat straw for efficient ethanol production using various solvents. *Biomass Bioenergy* **2017**, *100*, 10–16.
- (8) Ferreira, J. A.; Taherzadeh, M. J. Improving the economy of lignocellulose-based biorefineries with organosolv pretreatment. *Bioresour. Technol.* **2020**, 299, 122695.
- (9) Braz, D. S.; Mariano, A. P. Jet fuel production in eucalyptus pulp mills: Economics and carbon footprint of ethanol vs. butanol pathway. *Bioresour. Technol.* **2018**, 268, 9–19.
- (10) da Silva, A. R. G.; Errico, M.; Rong, B.-G. Evaluation of organosolv pretreatment for bioethanol production from lignocellulosic biomass: solvent recycle and process integration. *Biomass Convers. Biorefinery* **2018**, 8 (2), 397–411.
- (11) Smit, A. T.; Verges, M.; Schulze, P.; van Zomeren, A.; Lorenz, H. Laboratory-to Pilot-Scale Fractionation of Lignocellulosic Biomass

- Using an Acetone Organosolv Process. ACS Sustain. Chem. Eng. 2022, 10, 10503-10513.
- (12) Vaidya, A. A.; Murton, K. D.; Smith, D. A.; Dedual, G. A review on organosolv pretreatment of softwood with a focus on enzymatic hydrolysis of cellulose. *Biomass Convers. Biorefinery* **2022**, *12* (11), 5427–5442.
- (13) Awasthi, M. K.; Sindhu, R.; Sirohi, R.; Kumar, V.; Ahluwalia, V.; Binod, P.; Juneja, A.; Kumar, D.; Yan, B.; Sarsaiya, S.; et al. Agricultural waste biorefinery development towards circular bioeconomy. *Renew. Sust. Energy Rev.* **2022**, *158*, 112122.
- (14) Zandi Atashbar, N.; Labadie, N.; Prins, C. Modelling and optimization of biomass supply chains: a review. *Int. J. Prod. Res.* **2018**, *56* (10), 3482–3506.
- (15) Uludere Aragon, N. Z.; Parker, N. C.; VanLoocke, A.; Bagley, J.; Wang, M.; Georgescu, M. Sustainable land use and viability of biojet fuels. *Nat. Sustain.* **2023**, *6* (2), 158–168.
- (16) Roni, M. S.; Lin, Y.; Hartley, D. S.; Thompson, D. N.; Hoover, A. N.; Emerson, R. M. Importance of incorporating spatial and temporal variability of biomass yield and quality in bioenergy supply chain. *Sci. Rep.* **2023**, *13* (1), 6813.
- (17) Smit, A. T.; van Zomeren, A.; Dussan, K.; Riddell, L. A.; Huijgen, W. J. J.; Dijkstra, J. W.; Bruijnincx, P. C. A. Biomass Pre-Extraction as a Versatile Strategy to Improve Biorefinery Feedstock Flexibility, Sugar Yields, and Lignin Purity. ACS Sustain. Chem. Eng. 2022, 10, 6012–6022.
- (18) Smit, A. T.; Huijgen, W. J. J. Effective fractionation of lignocellulose in herbaceous biomass and hardwood using a mild acetone organosolv process. *Green Chem.* **2017**, *19* (22), 5505–5514.
- (19) Beaucamp, A.; Muddasar, M.; Amiinu, I. S.; Leite, M. M.; Culebras, M.; Latha, K.; Gutiérrez, M. C.; Rodriguez-Padron, D.; del Monte, F.; Kennedy, T.; et al. Lignin for energy applications-state of the art, life cycle, technoeconomic analysis and future trends. *Green Chem.* **2022**, *24*, 8193–8226.
- (20) Trano, S.; Corsini, F.; Pascuzzi, G.; Giove, E.; Fagiolari, L.; Amici, J.; Francia, C.; Turri, S.; Bodoardo, S.; Griffini, G.; Bella, F. Lignin as polymer electrolyte precursor for stable and sustainable potassium batteries. *ChemSusChem* **2022**, *15* (12), No. e202200294.
- (21) Lu, X.; Gu, X.; Shi, Y. A review on lignin antioxidants: Their sources, isolations, antioxidant activities and various applications. *Int. J. Biol. Macromol.* **2022**, *210*, 716–741.
- (22) Sternberg, J.; Sequerth, O.; Pilla, S. Green chemistry design in polymers derived from lignin: review and perspective. *Prog. Polym. Sci.* **2021**, *113*, 101344.
- (23) Li, W.; Sun, H.; Wang, G.; Sui, W.; Dai, L.; Si, C. Lignin as a green and multifunctional alternative of phenol for resin synthesis. *Green Chem.* **2023**, 25, 2241.
- (24) Duval, A.; Vidal, D.; Sarbu, A.; René, W.; Avérous, L. Scalable single-step synthesis of lignin-based liquid polyols with ethylene carbonate for polyurethane foams. *Mater. Today Chem.* **2022**, *24*, 100793.
- (25) Poveda-Giraldo, J. A.; Solarte-Toro, J. C.; Alzate, C. A. C. The potential use of lignin as a platform product in biorefineries: A review. *Renew. Sust. Energy Rev.* **2021**, *138*, 110688.
- (26) Gan, M. J.; Niu, Y. Q.; Qu, X. J.; Zhou, C. H. Lignin to value-added chemicals and advanced materials: extraction, degradation, and functionalization. *Green Chem.* **2022**, *24*, 7705–7750.
- (27) Tardy, B. L.; Lizundia, E.; Guizani, C.; Hakkarainen, M.; Sipponen, M. H. Prospects for the integration of lignin materials into the circular economy. *Mater. Today* **2023**, *65*, 122–132.
- (28) Smit, A. T.; Dezaire, T.; Riddell, L. A.; Bruijnincx, P. C. A. Reductive Partial Depolymerization of Acetone Organosolv Lignin to Tailor Lignin Molar Mass, Dispersity, and Reactivity for Polymer Applications. ACS Sustain. Chem. Eng. 2023, 11 (15), 6070–6080.
- (29) Smit, A. T.; Bellinetto, E.; Dezaire, T.; Boumezgane, O.; Riddell, L. A.; Turri, S.; Hoek, M.; Bruijnincx, P. C.; Griffini, G. Tuning the properties of biobased PU coatings via selective lignin fractionation and partial depolymerization. ACS Sustain. Chem. Eng. 2023, 11 (18), 7193–7202.

- (30) Firmanda, A.; Syamsu, K.; Sari, Y. W.; Cabral, J.; Pletzer, D.; Mahadik, B.; Fisher, J.; Fahma, F. 3D printed cellulose based product applications. *Mater. Chem. Front.* **2022**, *6* (3), 254–279.
- (31) Rojo, E.; Peresin, M. S.; Sampson, W. W.; Hoeger, I. C.; Vartiainen, J.; Laine, J.; Rojas, O. J. Comprehensive elucidation of the effect of residual lignin on the physical, barrier, mechanical and surface properties of nanocellulose films. *Green Chem.* **2015**, *17* (3), 1853–1866.
- (32) Shaghaleh, H.; Xu, X.; Wang, S. Current progress in production of biopolymeric materials based on cellulose, cellulose nanofibers, and cellulose derivatives. *RSC Adv.* **2018**, *8* (2), 825–842.
- (33) Zhou, Z.; Lei, F.; Li, P.; Jiang, J. Lignocellulosic biomass to biofuels and biochemicals: A comprehensive review with a focus on ethanol organosolv pretreatment technology. *Biotechnol. Bioeng.* **2018**, 115 (11), 2683–2702.
- (34) Scarica, C.; Suriano, R.; Levi, M.; Turri, S.; Griffini, G. Lignin functionalized with succinic anhydride as building block for biobased thermosetting polyester coatings. *ACS Sustain. Chem. Eng.* **2018**, *6* (3), 3392–3401.
- (35) Huang, H.; Xu, C.; Zhu, X.; Li, B.; Huang, C. Lignin-enhanced wet strength of cellulose-based materials: a sustainable approach. *Green Chem.* **2023**, 25, 4995.
- (36) Agustiany, E. A.; Rasyidur Ridho, M.; Rahmi, D. N. M.; Madyaratri, E. W.; Falah, F.; Lubis, M. A. R.; Solihat, N. N.; Syamani, F. A.; Karungamye, P.; Sohail, A.; et al. Recent developments in lignin modification and its application in lignin-based green composites: A review. *Polym. Compos.* **2022**, *43* (8), 4848–4865.
- (37) Li, W.; Tan, X.; Miao, C.; Zhang, Z.; Wang, Y.; Ragauskas, A. J.; Zhuang, X. Mild organosolv pretreatment of sugarcane bagasse with acetone/phenoxyethanol/water for enhanced sugar production. *Green Chem.* **2023**, 25 (3), 1169–1178.
- (38) Pals, M.; Lauberts, M.; Zijlstra, D. S.; Ponomarenko, J.; Arshanitsa, A.; Deuss, P. J. Mild organosolv delignification of residual aspen bark after extractives isolation as a step in biorefinery processing schemes. *Molecules* **2022**, *27* (10), 3185.
- (39) Kumaniaev, I.; Subbotina, E.; Sävmarker, J.; Larhed, M.; Galkin, M. V.; Samec, J. S. Lignin depolymerization to monophenolic compounds in a flow-through system. *Green Chem.* **2017**, *19* (24), 5767–5771.
- (40) Labauze, H.; Cachet, N.; Benjelloun-Mlayah, B. Acid-based organosolv lignin extraction from wheat straw: Kinetic and structural analysis. *Ind. Crops Prod.* **2022**, *187*, 115328.
- (41) Karlsson, M.; Giummarella, N.; Lindén, P. A.; Lawoko, M. Toward a Consolidated Lignin Biorefinery: Preserving the Lignin Structure through Additive-Free Protection Strategies. *ChemSusChem* **2020**, *13* (17), 4666–4677.
- (42) Karlsson, M.; Vegunta, V. L.; Deshpande, R.; Lawoko, M. Protected lignin biorefining through cyclic extraction: gaining fundamental insights into the tuneable properties of lignin by chemometrics. *Green Chem.* **2022**, 24 (3), 1211–1223.
- (43) Karlsson, M.; Romson, J.; Elder, T.; Emmer, Å.; Lawoko, M. Lignin Structure and Reactivity in the Organosolv Process Studied by NMR Spectroscopy, Mass Spectrometry, and Density Functional Theory. *Biomacromolecules* **2023**, 24 (5), 2314–2326.
- (44) Zijlstra, D. S.; Analbers, C. A.; de Korte, J.; Wilbers, E.; Deuss, P. J. Efficient mild organosolv lignin extraction in a flow-through setup yielding lignin with high β -O-4 content. *Polymers* **2019**, *11* (12), 1913.
- (45) Zijlstra, D. S.; Lahive, C. W.; Analbers, C. A.; Figueirêdo, M. B.; Wang, Z.; Lancefield, C. S.; Deuss, P. J. Mild organosolv lignin extraction with alcohols: the importance of benzylic alkoxylation. *ACS Sustain. Chem. Eng.* **2020**, *8* (13), 5119–5131.
- (46) Zhou, H.; Tan, L.; Fu, Y.; Zhang, H.; Liu, N.; Qin, M.; Wang, Z. Rapid nondestructive fractionation of biomass (≤ 15 min) by using flow-through recyclable formic acid toward whole valorization of carbohydrate and lignin. *ChemSusChem* **2019**, *12* (6), 1213−1221.
- (47) Zhou, H.; Xu, J. Y.; Fu, Y.; Zhang, H.; Yuan, Z.; Qin, M.; Wang, Z. Rapid flow-through fractionation of biomass to preserve labile aryl ether bonds in native lignin. *Green Chem.* **2019**, *21* (17), 4625–4632.

- (48) Castillo-Santos, K.; Aguirre-Alonso, R.; Rodríguez-Jimenes, G.; Robles-Olvera, V. J.; Salgado-Cervantes, M.; García-Alvarado, M. An optimization based algorithm for solving design problems of countercurrent multistage batch solid-liquid extractors for complex systems: Application to vanilla extract. *Comput. Chem. Eng.* **2016**, *89*, 53–61.
- (49) Lin, P.; Werner, J.; Ali, Z. A.; Bertucci, L.; Groppo, J. Kinetics and Modeling of Counter-Current Leaching of Waste Random-Access Memory Chips in a Cu-NH3-SO4 System Utilizing Cu (II) as an Oxidizer. *Materials* **2023**, *16* (18), 6274.
- (50) Zhang, B.; Gao, Z.; Liu, H.; Wang, W.; Cao, Y. Direct acid leaching of vanadium from stone coal. *High Temp. Mater. Process.* **2017**, 36 (9), 877–883.
- (51) Haghighi, H. K.; Moradkhani, D.; Salarirad, M. M. Separation of zinc from manganese, magnesium, calcium and cadmium using batch countercurrent extraction simulation followed by scrubbing and stripping. *Hydrometallurgy* **2015**, *154*, 9–16.
- (52) Feng, D.; Van Deventer, J. Oxidative pre-treatment in thiosulphate leaching of sulphide gold ores. *Int. J. Miner. Process.* **2010**, 94 (1–2), 28–34.
- (53) Ferreira, M. C.; Gonçalves, D.; Bessa, L. C.; Rodrigues, C. E.; Meirelles, A. J.; Batista, E. A. Soybean oil extraction with ethanol from multiple-batch assays to reproduce a continuous, countercurrent, and multistage equipment. *Chem. Eng. Process.* **2022**, *170*, 108659.
- (54) Joseph, P.; Ottesen, V.; Opedal, M. T.; Moe, S. T. Morphology of lignin structures on fiber surfaces after organosolv pretreatment. *Biopolymers* **2022**, *113* (9), No. e23520.
- (55) Lancefield, C. S.; Panovic, I.; Deuss, P. J.; Barta, K.; Westwood, N. J. Pre-treatment of lignocellulosic feedstocks using biorenewable alcohols: towards complete biomass valorisation. *Green Chem.* **2017**, 19 (1), 202–214.
- (56) Bergrath, J.; Rumpf, J.; Burger, R.; Do, X. T.; Wirtz, M.; Schulze, M. Beyond Yield Optimization: The Impact of Organosolv Process Parameters on Lignin Structure. *Macromol. Mater. Eng.* **2023**, 308, 2300093.
- (57) Wang, Z.; Qiu, S.; Hirth, K.; Cheng, J.; Wen, J.; Li, N.; Fang, Y.; Pan, X.; Zhu, J. Preserving both lignin and cellulose chemical structures: flow-through acid hydrotropic fractionation at atmospheric pressure for complete wood valorization. *ACS Sustain. Chem. Eng.* **2019**, 7 (12), 10808–10820.
- (58) Tian, G.; Xu, J.; Fu, Y.; Guo, Y.; Wang, Z.; Li, Q. High β -O-4 polymeric lignin and oligomeric phenols from flow-through fractionation of wheat straw using recyclable aqueous formic acid. *Ind. Crops Prod.* **2019**, *131*, 142–150.
- (59) Li, M.; Yoo, C. G.; Pu, Y.; Ragauskas, A. J. 31 P NMR chemical shifts of solvents and products impurities in biomass pretreatments. *ACS Sustain. Chem. Eng.* **2018**, *6* (1), 1265–1270.
- (60) Giummarella, N.; Pu, Y.; Ragauskas, A. J.; Lawoko, M. A critical review on the analysis of lignin carbohydrate bonds. *Green Chem.* **2019**, *21* (7), 1573–1595.
- (61) Narron, R. H.; Chang, H.-m.; Jameel, H.; Park, S. Soluble lignin recovered from biorefinery pretreatment hydrolyzate characterized by lignin-carbohydrate complexes. *ACS Sustain. Chem. Eng.* **2017**, 5 (11), 10763–10771.
- (62) Pongchaiphol, S.; Suriyachai, N.; Hararak, B.; Raita, M.; Laosiripojana, N.; Champreda, V. Physicochemical characteristics of organosolv lignins from different lignocellulosic agricultural wastes. *Int. J. Biol. Macromol.* **2022**, *216*, 710–727.